Anal Bioanal Chem (2007) 389:2217–2225
DOI 10.1007/s00216-007-1656-6

ORIGINAL PAPER

Determination of loratadine and pseudoephedrine sulfate in pharmaceuticals based on non-linear second-order spectrophotometric data generated by a pH-gradient flow injection technique and artificial neural networks

María J. Culzoni · Héctor C. Goicoechea

Received: 21 August 2007 / Accepted: 19 September 2007 / Published online: 23 October 2007

Abstract Loratadine (LOR) and pseudoephedrine sulfate (PES) were determined in pharmaceutical samples by using non-linear second-order data generated by a pH-gradient flow injection analysis (FIA) system with diode-array detection. Determination of both analytes was performed on the basis of differences between the acid–base and spectral features of each drug species. Non-linearities were detected by using both qualitative and quantitative tools. As a consequence of the non-linearity, a recently reported algorithm, artificial neural networks followed by residual bilinearization (ANN/RBL), was shown to furnish more satisfactory results. Recoveries of 99.7% (LOR) and 95.6% (PES) were obtained when analyzing a validation set containing unexpected components (the usual excipients found in pharmaceutical preparations). The average value obtained by implementation of the method on four replicates was compared with that obtained by a reference method based on HPLC (difference not significant; $p > 0.05$).

Keywords Loratadine · Pseudoephedrine · Pharmaceutical · Artificial neural networks · Second-order advantage

M. J. Culzoni · H. C. Goicoechea (✉)
Laboratorio de Desarrollo Analítico y Quimiometría (LADAQ),
Cátedra de Química Analítica I, Facultad de Bioquímica y
Ciencias Biológicas, Universidad Nacional del Litoral,
Ciudad Universitaria,
Santa Fe (S3000ZAA), Argentina
e-mail: hgoico@fbcb.unl.edu.ar

Abbreviations

U-PLS/RBL	Unfolded partial-least-squares/residual bilinearization
ANN/RBL	Artificial neural networks followed by residual bilinearization
HPLC	High-performance liquid chromatography
PARAFAC	Parallel-factor analysis
GRAM	Generalized rank-annihilation method
MCR–ALS	Multivariate curve resolution–alternating least squares
FIA	Flow injection analysis
DAD	Diode-array detector
SVD	Singular-value decomposition

Introduction

The combination of loratadine (LOR) and pseudoephedrine sulfate (PES) in medicinal products is effective in the relief of symptoms associated with seasonal allergic rhinitis accompanied by nasal congestion [1]. LOR is a nonsedating long-acting antihistamine belonging to the H-1 antagonist group; PES is used as an oral decongestant [1].

Few analytical applications for LOR and PES have been reported in the literature. Both analytes have been simultaneously determined in pharmaceutical preparations by derivative spectroscopy [2, 3] and high-performance liquid chromatography (HPLC) [4, 5]. Very recently, a manual pH-gradient spectrophotometric application on artificial samples has been reported with the aim of checking the capability of a newly developed chemometric algorithm [6]. Quantification of LOR and PES in biological fluids has also

been carried out by applying liquid chromatography coupled with mass spectrometry [7, 8].

Currently, second-order data are commonly being generated in analytical laboratories and used to solve more and more complex systems [9]. These data, when processed by suitable algorithms, give the analyst the second-order advantage, i.e. the possibility of analyzing any sample containing unexpected components that could be responsible for causing interferences [10].

Commonly employed second-order data are obtained by using:

1. a single instrument, such as a spectrofluorimeter (EEMs, excitation–emission matrices) or a diode-array spectrophotometer after spectral evolution of a chemical reaction (for example a kinetic or acid–base reaction); or
2. coupling or "hyphenating" two first-order instruments, for example tandem liquid chromatography–diode-array detection (LC–DAD), gas chromatography–mass spectrometry (GC–MS), GC–GC, MS–MS, etc. [10].

The analyst can use a large number of algorithms to deal with second-order data. Among those most often used, the following can be cited: parallel factor analysis (PARAFAC) [11], the generalized rank annihilation method (GRAM) [12], multivariate curve resolution–alternating least squares (MCR–ALS) [13], and unfolded partial-least-squares followed by residual bilinearization (U-PLS/RBL) [14]. These algorithms are of major relevance to the analysis of complex mixtures, because they achieve the second-order advantage. However, the analyst will be constrained by the structure of the data being managed. For example, the mentioned algorithms cannot be used when the recorded signals have a non-linear relationship with analyte concentration. Auspiciously, very recently a new algorithm—artificial neural networks followed by residual bilinearization (ANN/RBL)—was presented for dealing with non-linear data [15].

In this report, non-linear second-order data were generated by a pH-gradient flow injection analysis (FIA) system with diode-array detection. As a result, determination of both analytes was performed on the basis of the different acid–base and spectral features of each drug species. However, a clear non-linear relationship was observed between the concentration and absorbances measured in the studied range for both analytes, because one of the analytes (PES) is present at a relatively high concentration in comparison with the other (LOR). Therefore, classical second-order multivariate calibration methods could not be successfully applied. Instead, ANN/RBL was shown to be appropriate for training these non-linear spectroscopic data and successfully predicting analyte concentrations in the presence of unexpected constituents, thus achieving the important second-order advantage.

Theory

ANN modeling

The ANN architecture most commonly used for calibration applications consists of three layers with variable numbers of neurons [16]. The first corresponds to an input layer to accommodate the input data. The second is a hidden layer, whose number is adjusted on a trial-and-error basis. The last is an output layer with a single neuron, which yields the concentration of the analyte of interest in each sample. Both the input and hidden layers also include the so-called bias neurons, whose inputs are equal to 1. The common practice is to compress the input data into a reduced number (A) of principal components (PC) or scores. Thus, the number of input neurons equals A, where, in general, $A<<JK$ (number of sensors after the unfolding procedure). The value of A can be estimated, for example, by computing the percentage of variance explained by the principal components of the unfolded training data matrix (size $I\times JK$, I is the number of training samples), and selecting the first A PCs which explain more than a certain percentage (e.g., 99%) of the total variance.

Once the first A PCs are loaded into the A neurons of the input layer, the outputs are calculated for each training sample using a set of randomly selected initial weights which are transferred from layer to layer through a suitable transfer function [17], which currently is the sigmoidal transfer function $f(x) = 1/[1 + \exp(-x)]$. The weights are then modified according to the back-propagation methodology, which compares the ANN outputs with the nominal values of the analyte concentration in the training and monitoring samples. Two figures are obtained from these comparison:

1. the training root-mean-square error (RMSET), which is computed every training cycle, and allows the correction of the network weights which leads to a decrease of the RMSET; and
2. the RMSEM (M for monitoring), which simultaneously monitors the ANN performance by the results provided on an independent monitoring sample set.

Usually the net is trained during a number of epochs until a RMSEM value compatible with the noise level present in the system is reached. This value should correspond to a minimum in the RMSEM, in order to avoid overtraining [17]. Two important parameters for network training are the learning rate, which tends towards a fast, steepest-descent convergence, and the momentum, a long-range function preventing the solution from being trapped in local minima. These parameters are usually tuned around a value of 0.5, also by trial and error. The final set of weights is stored for future prediction on new samples.

RBL procedure

The training/prediction scheme works properly provided the new test samples do not have unexpected components. If yes, its scores will not be suitable for analyte prediction using the trained ANN. In this case, it is necessary to resort to a technique which marks the new sample as an outlier, indicating that further actions are necessary before ANN prediction, and then isolates the contribution of the unexpected component from that of the calibrated analytes, in order to recalculate appropriate scores for the test sample. This can be accomplished through PC analysis (PCA), since the sample will be considered as an outlier if the residuals of the PC analysis of $\mathbf{X}_u$ (s_p in Eq. 1) are abnormally large in comparison with the typical instrumental noise:

$$\begin{aligned} s_p &= \|\mathbf{e}_p\| \Big/ (JK - A)^{1/2} \\ &= \|\mathrm{vec}(\mathbf{X}_u) - \mathbf{P}\,\mathbf{P}^T \mathrm{vec}(\mathbf{X}_u)\| \Big/ (JK - A)^{1/2} \\ &= \|\mathrm{vec}(\mathbf{X}_u) - \mathbf{P}\,\mathbf{t}_u\| \Big/ (JK - A)^{1/2} \end{aligned} \quad (1)$$

where $\|.\|$ indicates the Euclidean norm, $\mathbf{P}$ is the matrix containing the first A loadings obtained by applying PCA to the unfolded training data, $\mathbf{t}_u$ is the vector of test sample scores, and vec() indicates the unfolding operation. The sizes of the relevant arrays in Eq. (1) are as follows: $\mathbf{e}_p$ and vec($\mathbf{X}_u$), $JK\times1$; $\mathbf{X}_u$, $J\times K$; $\mathbf{P}$, $JK\times A$ and $\mathbf{t}_u$, $A\times1$. If s_p is indeed large, then RBL can be employed to model the presence of unexpected sample components, decomposing the signal for a test sample containing unexpected components into two parts: one modeled using the calibration latent variables ($\mathbf{X}_{mod}$) and the remaining part which cannot be modeled ($\mathbf{X}_{unmod}$) with these variables.

In PCA, the modeled part can be expressed as a function of the calibrated latent variables $\mathbf{P}$ and the unknown sample score $\mathbf{t}_u$, and, hence:

$$\mathrm{vec}(\mathbf{X}_u) = \mathbf{P}\,\mathbf{t}_u + \mathbf{e}_{mod} + \mathrm{vec}(\mathbf{X}_{unmod}) \quad (2)$$

where $\mathbf{e}_{mod}$ is the vector of residuals not fitted to $\mathbf{X}_{mod}$ by the PCA model with A principal components (notice the relationship $\mathbf{e}_p=\mathbf{e}_{mod}+\mathrm{vec}(\mathbf{X}_{unmod})$). In the absence of unexpected components, $\mathbf{e}_{mod}=\mathbf{e}_p$, which will contain elements of the order of the instrumental noise. However, if anything having a bilinear structure is present in $\mathbf{X}_{unmod}$ which rises above the noise level, it can be modeled using PCA, which is normally carried out through singular-value decomposition (SVD). This allows one to estimate profiles for the unexpected components ($\mathbf{b}_{unx}$ and $\mathbf{c}_{unx}$) and hence Eq. (2) can be represented as:

$$\mathrm{vec}(\mathbf{X}_u) = \mathbf{P}\,\mathbf{t}_u + \mathrm{vec}\left[g_{unx}\mathbf{b}_{unx}(\mathbf{c}_{unx})^T\right] + \mathbf{e}_u \quad (3)$$

The RBL procedure consists in keeping the matrix $\mathbf{P}$ in Eq. (3) constant at the calibration value, and varying $\mathbf{t}_u$ in order to minimize the norm of the residual vector $\mathbf{e}_u$ ($\|e_u\|$). During the minimization, profiles for the unexpected components are continually updated through SVD of a matrix obtained after reshaping $\mathbf{e}_p$ (Eq. 1):

$$(g_{unx}, \mathbf{b}_{unx}, \mathbf{c}_{unx}) = \mathrm{SVD}_1(\mathbf{E}_p) \quad (4)$$

where $\mathbf{E}_p$ is the $J\times K$ matrix obtained after reshaping the $JK\times1$ $\mathbf{e}_p$ vector, and SVD_1 indicates taking the first principal component. It is important to notice that it is in Eq. (4) where the reshaping operation of $\mathbf{e}_p$ folds the (transformed) data into a matrix, and this permits the achievement of the second-order advantage, even when the data are unfolded for calibration purposes. RBL is thus only possible with second-order data, which can be meaningfully arranged into a matrix. It should be remarked that RBL will succeed provided $\mathbf{X}_{unmod}$ does not contain spectral components which are collinear with those in $\mathbf{X}_{mod}$.

Minimization of $\|\mathbf{e}_u\|$ can be carried out starting with a $\mathbf{t}_u$ vector as given by the projection of the test sample responses on the space spanned by the calibration A principal components. Minimization of residuals is performed through the Gauss–Newton approach. It is carried out until the difference between successive values of $\|\mathbf{e}_u\|$ is lower than certain previously set tolerance limit. Repeating the minimization a number of times for a given sample did not produce significantly different results.

Should it be necessary to consider a larger number of unexpected components (N_{unx}) in the SVD analysis of $\mathbf{E}_p$ (Eq. 5), then N_{unx} can be assessed by comparing the final residuals s_u with the instrumental noise level, with s_u given by:

$$s_u = \|\mathbf{e}_u\| \Big/ [JK - (A + N_{unx})]^{1/2} \quad (5)$$

where $\mathbf{e}_u$ is from Eq. (3). Typically, a plot of s_u computed for trial values of N_{unx} will show decreasing values, starting at s_p when $N_{unx}=0$, until it stabilizes at a value compatible with the experimental noise, allowing location of the correct number of unexpected components. If $N_{unx}>1$, the profiles provided by the SVD analysis of $\mathbf{E}_p$ would not resemble the true profiles for the unexpected components, because the principal components are restricted to being orthonormal. While the first component may resemble a chemical constituent in the sample, the remaining ones will not be comparable to true spectra.

Finally, once the correct test sample scores $\mathbf{t}_u$ have been found, they are introduced into the input neurons of the trained ANN, providing the analyte concentration as output. Complementarily, the test sample scores obtained before and after the RBL procedure can be plotted in a score plot together with the calibration sample scores in order to

visualize if the test sample data have been freed from the effect of the interferents [6].

U-PLS/RBL

The U-PLS/RBL methodology has already been described in detail in the relevant literature [14]. Since it is able to cope with mild deviations from linearity by including additional factors in the model, it was one of the chosen second-order methodologies applied to resolution with the aim of further comparing the prediction results with those obtained from ANN/RBL.

MCR–ALS

The well-known MCR–ALS algorithm [13, 18] was also employed to manage the present analytical problem. For that purpose, simultaneous analysis of several sets of correlated $\mathbf{D}_i$ sub-matrices of spectra recorded during the flow injection process, arranged as column-wise augmented **D** data matrices, was performed.

Before starting resolution, determination of the number of contributions to each **D** data matrix was performed by applying singular-value decomposition (SVD). The $\mathbf{S}^T$-type initial estimates were then built by selection of the purest spectra based on SIMPLISMA [19].

Given **D** and $\mathbf{S}^T$, appropriate constraints (i.e. non-negativity for spectra and concentration profiles and correspondence between common species in different runs) were implemented to drive the iterative optimization to the right solution.

Experimental

Apparatus

The single-channel FIA system and the chromatographic procedure were developed using five modules (degasser, pump, injection valve, autosampler and, detector) of an Agilent 1100 Series instrument (Agilent Technologies, Waldbronn, Germany).

The flow injection manifold which is pictorially illustrated in Fig. 1 consisted of a carrier channel of 0.2 mol L^{-1} acetic acid (pH=3.0) at a flow rate of 0.2 mL min^{-1}, in which injections of 100 μL sample solution prepared in 0.2 mol L^{-1} acetate buffer (pH=7.0) were performed. The pH gradient was generated in a 200 cm×0.12 mm i.d mixing coil and was shown to be highly reproducible run-to-run. For each FI peak, spectra were registered in the range 200–300 nm each 1 nm at regular time intervals of 2 s for 180 s. Therefore, matrices of size 444×101 per sample were generated, although region selections (in both dimensions) were applied before multivariate calibration.

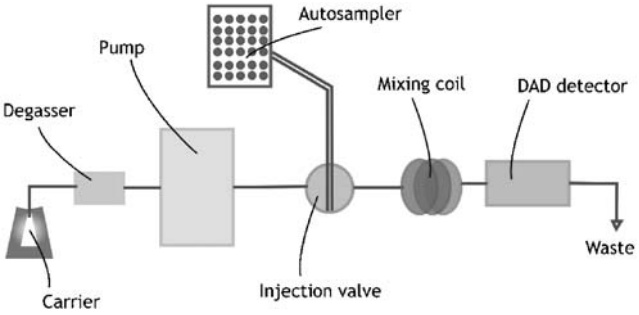

Fig. 1 Flow injection manifold

HPLC measurements were carried out on a 5-μm Zorbax Eclipse XDB-C18 column (4.6×150 mm). All chromatograms were recorded at room temperature, using a mixture of 60% (methanol–H_2O–phosphoric acid–ammonium dihydrogen phosphate 220:300:2:3 g, *v*/*v*/*v*/*w*) and 40% acetonitrile as mobile phase flowing at 1 mL min^{-1} with ultraviolet detection at 247 nm [2].

Software

All multivariate algorithms were implemented in Matlab 7.1 [20]. The MCR–ALS algorithms were downloaded from the Multivariate Curve Resolution web page: http://www.ub.es/gesq/mcr/mcr.htm. Routines for applying ANN/RBL and U-PLS/RBL are available from the authors on request; these include a graphical user interface which also provides access to a variety of second-order multivariate methodologies of the type already described for the first-order multivariate calibration [21]. Statgraphics Plus 5.1 software was used for all statistical analysis [22].

Reagents and solutions

All experiments were performed with analytical-reagent grade chemicals. Milli Q water was used for all solutions. LOR and PES standards were kindly provided by Química Montpellier, Buenos Aires, Argentina. Stock solutions of LOR (0.6203 g L^{-1}) and PES (6.0164 g L^{-1}) were prepared by dissolving each standard in HCl 0.1 mol L^{-1}. A solution of the excipients usually present in the commercial sample—propylene glycol, sorbitol, anhydrous citric acid, sodium benzoate, and sucrose—was also prepared in water, at concentrations corresponding to their known value in commercial samples.

Two solutions prepared from glacial acetic acid (Cicarelli, San Lorenzo, Argentina) and NaOH (Cicarelli, San Lorenzo, Argentina) were employed to create a double on-line pH gradient. A 0.2 mol L^{-1} acetic acid solution was prepared for use as carrier stream and 0.2 mol L^{-1} acetate buffer solution was used for dilution of the samples.

Experimental calibration and validation sets

A set of 25 samples corresponding to a five-level full-factorial design was prepared for calibration. Well-defined non-linear relationships were observed between the concentrations and absorbances measured in the studied ranges of 6.66–10.00 mg L^{-1} and 80.00–120.00 mg L^{-1} for LOR and PES, respectively (see below).

A validation set corresponding to a central composite design containing nine samples at different concentrations from those employed for calibration was also built for monitoring the ANN training.

An additional six-sample set was built for prediction requiring the second-order advantage. These samples were employed neither for training nor for monitoring of the ANN. They comprised mixtures of appropriate amounts of stock solutions of LOR and PES, also containing excipients usually present in the commercial samples at their known concentrations.

All samples were prepared in 2.00-mL volumetric flasks, diluted to volume with 0.2 mol L^{-1} acetate buffer and injected twice into the FIA system.

Sample

The analyzed sample was Decidex Plus Oral Solution (Roemmers, Argentina). This pharmaceutical contains 1.0 g L^{-1} LOR and 12.0 g L^{-1} PES and was diluted 1:120 with 0.2 mol L^{-1} acetate buffer in volumetric glassware before analysis.

Chromatographic procedure for real samples

Working solutions of LOR and PES were prepared by dissolving accurately known amounts of each standard in mobile phase and diluting in the same solvent to concentrations of 20 and 238 μg mL^{-1}, respectively. Real samples were diluted 1:50 in mobile phase. All solutions were filtered through a 0.45 μm membrane filter before injection of 20 μL. HPLC measurements were then performed as described above. Finally, peak areas were recorded to calculate concentrations in samples.

Results and discussion

Detection of nonlinearity

As a consequence of the high concentration difference between LOR and PES in the analyzed commercial sample, the dilution required to perform the determination of both analytes simultaneously introduces nonlinearities in the more concentrated analyte (PES) but may also lead to deviations from the linear absorbance–concentration range for the less concentrated drug (LOR).

In order to detect the presence of nonlinearity both qualitative and quantitative detection tools were implemented on spectra selected from the maximum FIA peak, i.e. first-order data were used to perform the following analysis. Initially, the most universal diagnostic plot, i.e. Mallows augmented partial residual plot (APaRP), was built for each analyte to assess a possible quadratic relationship between some of the first factors and the concentration [23]. For that purpose, the vector **y** which contains the individual analyte concentrations was regressed against the first A PLS-1 factors (**LV**) of the data matrix and the square of the first **LV** [24]:

$$y_i = b_0 + b_1 LV_{1i} + ... + b_A LV_{Ai} + b_{11}(LV_{1i})^2 + \mathbf{e}_{APaRPi} \quad (6)$$

where e_{APaRPi} are the elements of a vector containing the residuals of the APaRP fitting ($\mathbf{e}_{APaRP}$). The relevant plot was then obtained by plotting the sum $[\mathbf{e}_{APaRP}+b_1\mathbf{LV}_1+b_{11}(\mathbf{LV}_1)^2]$ against $\mathbf{LV}_1$ [24]. In the present case, the APaRP plots were constructed including the six first **LV**s into the model, for both analytes. Observation of Fig. 2a,b reveals evidence of mild non-linear behavior for LOR in contrast with a considerable quadratic non-linear pattern for PES, present in the data set.

To quantitatively evaluate the degree of non-linearity, examinations were carried out by applying both Runs and Durbin–Watson tests. The former examines the number of series of consecutive residuals with the same sign (runs), indicating a trend when long runs occur based on the calculation of the indicator z [24]:

$$z = (u - \sigma + 0.5)/\sigma \quad (7)$$

where u is the number of runs, and:

$$\mu = 1 + 2n_+n_-/(n_+ + n_-) \quad (8)$$

$$\sigma^2 = 2n_+n_-(2n_+n_- - n_+ - n_-)\Big/\left[(n_+ + n_-)^2(n_+ + n_- - 1)\right] \quad (9)$$

where n_+ and n_- are the number of positive and negative residuals. Non-linearity is present when z exceeds the critical value of 1.96 (at 95% confidence level). The latter test considers the null hypothesis (H_0) that there is no correlation between the successive residuals, versus the alternative hypothesis that the correlation exists, by computing the statistic d [25]:

$$d = \frac{\sum_{i=2}^{n}(e_i - e_{i-1})^2}{\sum_{i=1}^{n} e_i^2} \quad (10)$$

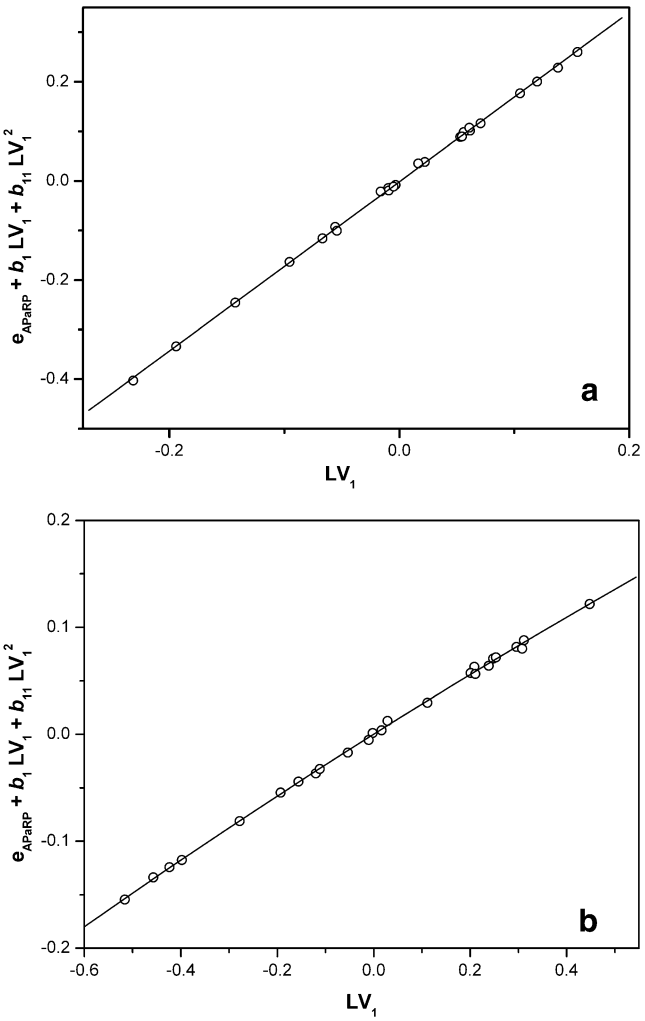

Fig. 2 Mallows augmented partial residual plot (APaRP) for LOR (**a**) and PES (**b**) when the six first LVs are included in the model for each

where e_i is a given residual, and e_{i-1} is the preceding one. Comparison of d with the two critical values d_L (lower) and d_U (upper), leads to the following conclusions:

1. if $d<d_L$ the null hypothesis is rejected, indicating correlation between residuals;
2. if $d_L<d<d_U$ the test is inconclusive; and
3. if $d>d_U$ the correlations are considered to be negligible.

As can be seen, the quantitative results presented in Table 1 confirm the APaRP plots conjecture, suggesting the presence of mild non-linearity for LOR and strongly supporting the non-linear pattern followed by PES.

On the basis of the previously described analysis, we can clearly state that the present analytical problem is non-linear and should be treated with appropriate second-order methodology able to cope with this behavior. Because of this, ANN/RBL was chosen, although PLS/RBL and MCR–ALS were also applied.

Determination of the ANN architectures

Optimization of the ANNs was performed by trial and error following two different strategies to set the initial number of input nodes. The stepwise addition approach consisting of starting with a deliberately small number of input variables (i.e. the first few PCs) and adding new variables one at a time until the monitoring and/or prediction performance of the net no longer improves [17], was applied to find the most appropriate net for LOR. On the other hand, the stepwise elimination approach was more convenient for establishing the best net for PES, starting with a deliberately large number of input variables and gradually removing some of them until the monitoring and/or prediction performance of the net stops improving [17]. Besides, a number of hidden neurons ranging from one to nine were used to train the nets for each trial number of input neurons. Parameters for all nets showing acceptable RMSET and RMSEM were stored in order to be tested subsequently.

Therefore, in order to assess the robustness of the ANN results, the best five models for each system were sequentially applied to prediction in the test samples. Table 2 shows the training parameters for the five best nets obtained for each analyte. The percentage recovery of the test set predictions gathered by applying all nets in resolution were analyzed with both the Bartlett and Tukey HSD (honestly significantly different) statistical tests [25].

The Bartlett's test was used to verify homogeneity of variances across each group of predictions. Because both calculated p-values, i.e. 0.54 and 0.82 for LOR and PES, respectively, are greater than the critical value of 0.05, there is no significant difference between variances when test samples are predicted with any of the five considered nets. Furthermore, it was established that there is no difference between the means obtained for each analyte when all pairwise comparisons among means were analyzed with Tukey's test at a confidence level of 95% (Fig. 3a,b).

On the basis of the latter evidence and on the similar RMSET and RMSEM between each group of selected nets, shown in Table 2, we can conclude that the whole tested

Table 1 Results from the Runs and Durbin–Watson tests applied to the APaRP plots to evaluate the degree of non-linearity

Component	Runs test		Durbin–Watson test	
	z value[a]	Conclusion	d value[a]	Conclusion
LOR	2.36	Non-linear	1.64	Inconclusive
PES	7.33	Non-linear	1.19	Non-linear

[a] The critical z and d values for the Runs and Durbin–Watson tests at $\alpha=0.05$ are $z_{crit}=1.96$, $d_L=1.32$, and $d_U=1.92$

Table 2 ANN parameters corresponding to training procedure for loratadine and pseudoephedrine sulfate

Parameter[a]	Value				
Loratadine					
Architecture[b]	4-6-1	4-7-1	4-8-1	5-8-1	5-9-1
Training cycles[c]	2953	1575	1285	1598	1182
Absolute (mg L^{-1}), relative (%) RMSET	0.41, 4.9	0.44, 5.4	0.44, 5.3	0.46, 5.5	0.47, 5.6
Absolute (mg L^{-1}), relative (%) RMSEM	0.27, 3.3	0.26, 3.1	0.29, 3.5	0.26, 3.2	0.41, 5.0
Average recovery (%)[d]	103.3(7)	105.3(8)	99.7(5)	98.6(6)	103.5(7)
Pseudoephedrine sulfate					
Architecture[b]	8-9-1	8-8-1	8-7-1	7-7-1	7-5-1
Training cycles[c]	681	1520	3000	1423	1402
Absolute (mg L^{-1}), relative (%) RMSET	0.79, 0.79	0.76, 0.76	0.72, 0.72	0.90, 0.90	0.78, 0.78
Absolute (mg L^{-1}), relative (%) RMSEM	2.0, 2.0	1.9, 1.9	1.8, 1.8	1.7, 1.7	1.7, 1.7
Average recovery (%)[d]	91.2(3)	95.3(4)	95.6(5)	93.1(4)	91.9(4)

[a] RMSE, root mean square error; T, training; M, monitoring. Relative percentage errors are calculated with respect to the mean calibration concentration

[b] The architecture is given as input, hidden, and output neurons

[c] Learning rate and momentum equal to 0.5

[d] Average of twelve determinations, standard deviation in parentheses

nets could be used to suitably deal with the present analytical system. However, we decided to work with those of architectures 4-8-1 and 8-7-1 for LOR and PES respectively, supported on the highest percentage recovery obtained when prediction of the test samples were done using them (Table 2). As can be noted, the more complex architecture necessary to model PES is another fact supporting the conclusions obtained from the non-linearity analysis (see above).

Multivariate calibration results

Test samples

Tables 3 and 4 show the results obtained for LOR and PES, respectively, when the test samples were analyzed. With respect to U-PLS/RBL, six calibration latent variables were estimated to be adequate by resorting to cross-validation [26], indicating that additional PLS latent variables should be considered with the intention of compensating for non-linearity. Three unexpected components were also necessary to decrease the prediction residuals, until they stabilized at a value compatible with the instrumental noise. On the other hand, the SVD analysis detected five components for suitable application of MCR–ALS. As can be seen, better prediction results and statistical parameters are achieved when the resolution is carried out with ANN/RBL, with one unexpected component for LOR and two for PES. Interestingly, results furnished when applying both linear methods to the non-linear system (PES) show a remarkable difference from those obtained by ANN/RBL (although better for MCR–ALS). Anyway, the recoveries obtained are different from the agencies' suggested acceptable range (95–105%) [27]. On the other hand, acceptable predictions for LOR are obtained by applying the three algorithms, although a high dispersion of the results is evident for the linear methods. Hence, the application

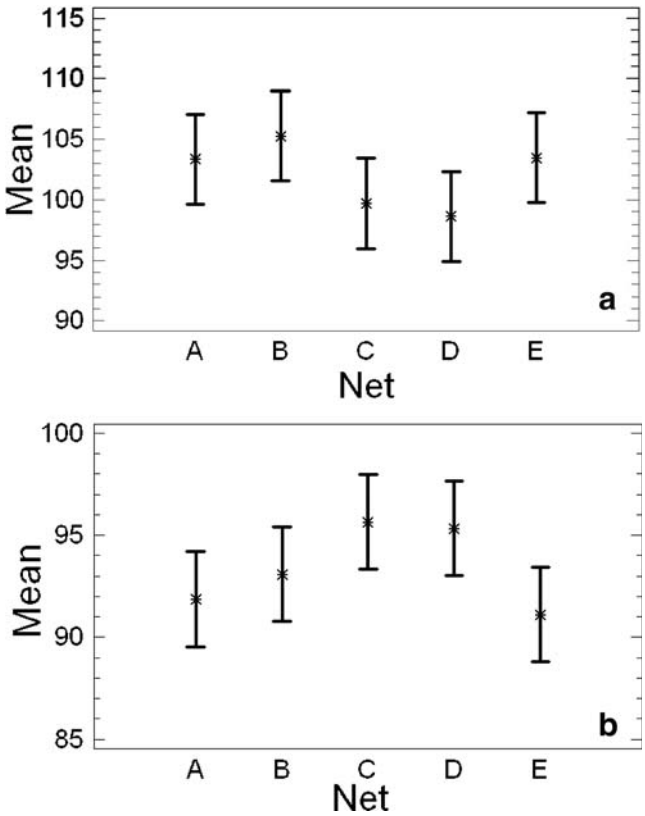

Fig. 3 Means and 95.0% Tukey HSD intervals against nets for (**a**) LOR, for the following architectures: A=4-6-1, B=4-7-1, C=4-8-1, D=5-8-1, and E=5-9-1, and (**b**) PES, for the following architectures: *A*=8-9-1, *B*=8-8-1, *C*=8-7-1, *D*=7-7-1, and *E*=7-5-1

Table 3 Test concentration and prediction results using PLS/RBL, MCR–ALS, and ANN/RBL for LOR

Sample	Actual (mg L^{-1})	Predicted (mg L^{-1})[a]		
		PLS/RBL[b]	MCR–ALS[c]	ANN/RBL[d]
1	8.33	8.62	9.97	8.27
2	7.50	8.52	8.84	8.11
3	9.16	9.54	9.83	9.00
4	7.50	7.01	7.24	7.14
5	9.16	8.78	8.92	9.32
6	8.33	7.83	7.71	7.98
Average recovery (%)[e]		100.8(8)	105.2(12)	99.7(5)
RMSEP (mg L^{-1}), REP (%)[f]		0.56, 6.7	0.95, 11.4	0.33, 4.0

[a] Average of the two injections into the FIA system for each sample
[b] Number of latent variables = 6 (established by leave-one-out cross-validation); number of unexpected components = 3
[c] Number of components = 5 (established by SVD)
[d] Number of unexpected components = 1
[e] Standard deviation in parentheses
[f] RMSEP = root mean square error of prediction; REP = relative error of prediction

of ANN/RBL can be recommended for the simultaneous determination of LOR and PES in real pharmaceutical samples.

Real samples

Finally, with the purpose of testing the applicability of the investigated method, the analysis of a real sample (four replicates) was performed by ANN/RBL, and the results were compared with those obtained by the HPLC method [2]. In the case of LOR, the average prediction obtained by ANN/RBL was 0.95 g L^{-1} (95.0% of the labeled amount). This concentration is statistically comparable with that obtained using the reference HPLC-based method (0.94 g L^{-1}, or 94.0% of the labeled amount), on the basis of an independent *t*-test. The latter was performed over the results of four replicates processed with each method yielding a probability of 0.57 at a confidence level of 95%. With respect to PES, the average prediction obtained by ANN/RBL was 11.29 g L^{-1} (94.1% of the labeled amount), which is also equivalent to the result provided by HPLC (11.57 g L^{-1}, or 96.4% of the labeled amount) furnishing a *p*-value of 0.42. Finally, U-PLS/RBL and MCR–ALS were also implemented for quantitation of the real sample. The differences between average values were significant, with $p<0.05$ for both algorithms (LOR and PES). These results are a good match with those obtained from analysis of the validation samples.

Table 4 Test concentration and prediction results using PLS/RBL, MCR–ALS, and ANN/RBL for PES

Sample	Actual (mg L^{-1})	Predicted (mg L^{-1})[a]		
		PLS/RBL[b]	MCR–ALS[c]	ANN/RBL[d]
1	114.10	102.51	122.42	104.13
2	90.00	83.67	97.12	82.80
3	90.00	84.48	94.80	84.96
4	110.00	93.80	124.68	113.44
5	110.00	95.66	110.30	110.15
6	100.00	87.81	102.86	92.93
Average recovery (%)[e]		89.5(3)	106.2(5)	95.6(5)
RMSEP (mg L^{-1}), REP (%)[f]		11.7, 11.4	7.8, 7.6	6.3, 6.1

[a] Average of the two injections into the FIA system for each sample
[b] Number of latent variables = 6 (established by leave-one-out cross-validation); number of unexpected components = 3
[c] Number of components = 5 (established by SVD)
[d] Number of unexpected components = 2
[e] Standard deviation in parentheses
[f] RMSEP = root mean square error of prediction; REP = relative error of prediction

Conclusions

A pH-gradient flow injection analysis (FIA) system with diode-array detection can be used to generate second-order data that can be conveniently managed for simultaneous determination of loratadine and pseudoephedrine in pharmaceuticals.

Owing to the high concentration difference between both active principles in commercial samples, a nonlinear relationship arises between the concentration and the instrumental signal for the more concentrated analyte (PES). This fact results in the application of ANN to obtain the second-order advantage. ANN is a powerful tool able to furnish better predictions and figures of merit than those provided by two well established linear algorithms, MCR–ALS and U-PLS/RBL.

In the light of these results, the present methodology can be recommended for quality-control analysis of LOR and PES in pharmaceuticals in routine laboratories.

Acknowledgment Financial support from Universidad Nacional del Litoral and Consejo Nacional de Investigaciones Científicas y Técnicas (CONICET) is gratefully acknowledged. M.J.C. thanks CONICET for a fellowship.

References

1. Brunton L (2005) In: Lazo J, Parker K (eds) Goodman and Gilman's The pharmacological basis of therapeutics. McGraw–Hill Professional, New York
2. Mabrouk MM, El-Fatatry HM, Hammad S, Aziz A, Wahbi AAM (2003) J Pharm Biomed Anal 33:597–604
3. Onur F, Yucesoy C, Dermis S, Kartal M, Kokdil G (2000) Talanta 51:269–279
4. Sane RT, Francis M, Khedkar S, Pawar S, Moghe A (2001) Indian Drugs 38:436–438
5. Vasudevan M, Ravisankar S, Sathiyanarayanan A, Chandan RS (2001) Indian Drugs 38:276–278
6. Culzoni MJ, Damiani PC, García-Reiriz A, Goicoechea HC, Olivieri AC (2007) Analyst 132:654–663
7. Naidong W (2003) J Chromatogr B 796:209–224
8. Gergov M, Ojanpera I, Vuori E (2003) J Chromatogr B 795:41–53
9. Escandar GM, Faber NM, Goicoechea HC, Muñoz de la Peña A, Olivieri AC, Poppi RJ (2007) Trends Anal Chem 26:752–764
10. Booksh KS, Kowalski BR (1994) Anal Chem 66:782A
11. Bro R (1997) Chemom Intell Lab Syst 38:149–171
12. Sanchez E, Kowalski BR (1986) Anal Chem 58:496–499
13. De Juan A, Casassas E, Tauler R (2002) In: Myers (ed) Encyclopedia of analytical chemistry, vol 11. Wiley, Chichester
14. Olivieri AC (2005) J Chemom 19:253–265
15. Olivieri AC (2006) J Chemom 20: 1–10
16. Despagne F, Massart DL (1998) Analyst 123:157R–178R
17. Zupan J, Gasteiger J (1999) Neural networks in chemistry and design. Wiley, New York
18. Tauler R (1995) Chemom Intell Lab Syst 30:133–146
19. Windig W, Guilment J (1991) Anal Chem 63:1425–1432
20. Matlab 7.1 (2005) The MathWorks Inc., Natick, Massachusetts, USA
21. Olivieri AC, Goicoechea HC, Iñon FA (2004) Chemom Intell Lab Syst 73:189–197
22. Statgraphics Plus (1994–2000) Statistical Graphics Corp., Herndon, Virginia, USA
23. Center V, de Noord OE, Massart DL (1998) Anal Chim Acta 376:153–168
24. Drapper NR, Smith H (1981) Applied regression analysis, 2nd edn. Wiley, New York
25. Montgomery DC (1991) Design and analysis of experiments. Wiley, New York
26. Haaland DM, Thomas EV (1988) Anal Chem 60:1193–1202
27. AOAC (1993) Peer-verified method program, manual on policies and procedures. AOAC, Arlington, VA, USA